THERMODYNAMIC AND HEAT TRANSFER ANALYSIS OF COOLING TECHNOLOGIES: A COMPARATIVE STUDY

W. R. I. Novais[a],
E. P. Cerqueira[a],
B. Narváez-Romo[a,b],
and J. R. Simões-Moreira[a]

[a]University of São Paulo
SISEA - Renewable and Alternative Energy Systems Lab.
Mechl. Eng. Department
Escola Politécnica
Av. Professor Mello Moraes, 2231
CEP 05508-030, São Paulo, São Paulo, Brazil
wellorzzon.novais@usp.br
erickcerqueira@usp.br
betonarmo@usp.br
jrsimoes@usp.br
[b]Universidad Pontificia Bolivariana
Grupo de Energía y Termodinámica
Facultad de Ingeniería Mecánica
Circular 1 No. 70-01, Medellín, Colombia

Received: Mar 03, 2022
Revised: Mar 31, 2022
Accepted: Mar 31, 2022

ABSTRACT

Refrigeration systems applications are broadly used in food and drug conservation and in air conditioning systems. Commercial buildings may demand as much as 80% of total electrical power just for powering the air-conditioning system based on conventional vapor compression refrigeration systems (VCRS), which contributes to reach peak demands on the electrical distribution network that could cause an unstable condition. Implementing absorption refrigeration systems (ARS) to produce cooling effects driven by thermal energy could decrease that power demand. Thermodynamic models of these systems can be found in the literature with a variety of working fluids and also integrated with other cycles such as power generation plants. However, a few previous analyses have a direct comparison between ARS and VCRS at the same operational conditions. Thus, the current study aims to simulate and compare two different refrigeration technologies: single stage ammonia-water absorption refrigeration system and vapor compression refrigeration system working with refrigerants R-134a and R-717. Thermodynamic simulation was carried out by evaluating heat transfer rates in the main devices, coefficients of performance, and specific areas of evaporator and condenser. As evaporator temperature decreases from 10°C to -20°C, ARS requires 16.9 kW or 67.5% more heat in generator and COP decreased from 0.601 to 0.359. Utilizing the same comparison parameter, VCRS needed 3.26-3.54 kW or 154-160% more compressor power, depending on refrigerant used, and COP decreased from 6.77 to 2.60 with R-134a and 7.07 to 2.79 using R-717 at the same condensation temperature (40°C). Compared to ARS, condenser specific area required for VCRS is smaller, evaporator is twofold smaller when using R-134a, and is equal when using R-717. Those results can justify the usage of ARS in facilities with high amount of waste heat, mainly on applications working with lower evaporator temperatures.

Keywords: absorption refrigeration system, compression refrigeration system, thermodynamic simulation, heat transfer, ammonia-water

NOMENCLATURE

A	area, m²
COP	Coefficient of Performance
NTU	Number of Transfer Units
$\dot{Q}$	heat transfer rate, kW
$\dot{W}$	work power, kW

Subscripts

ARS	Absorption Refrigeration System
com	compressor
dev	device
eva	evaporator
gen	generator
spc	specific
VCRS	Vapor Compression Refrigeration System

INTRODUCTION

Refrigeration systems are applied in food or drug conservation and air-conditioning to increase thermal comfort in offices and other commercial environments. Vapor compression refrigeration systems (VCRS) are used mainly for convenience, since this system only requires the largely available electrical power. However, the air-conditioning alone can consume as much as 60% to 80% of building electrical power, in agreement to Kassas (2015). This high power consumption can cause electrical distribution network peaks, according to Wells and Haas (2004) and Opoku *et al.* (2019). An absorption refrigeration system (ARS) uses far less electrical power, depending mostly on thermal energy to drive the system. Industries can benefit from the residual waste heat rejected by some processes to power their cooling systems and increase their technical and economic viability.

In the literature, some researches were developed to study the thermodynamics involving ARS and VCRS. Narváez-Romo *et al.* (2017) made an extensive review of heat and mass transfer correlations in ARS using ammonia-water or water-lithium bromide working pairs. Braga Martins and Figueiredo (2019) simulated a system with 7.1 kW of cooling capacity

adopting global heat transfer rate and experimental data to improve the system coefficient of performance (COP) by up to 31%. In a similar way, Hmida *et al.* (2019) defined a model to analyze the energy transfer and thermodynamic characteristics of a single effect ARS with 8 kW of refrigeration capacity installed in a room, achieving system COP of 0.72-0.74 when temperatures of generator and evaporator were 120°C and 2°C, respectively. Narváez-Romo and Simões-Moreira (2019) and Narváez-Romo *et al.* (2020) presented an analysis of heat transfer in the absorption process. Narváez-Romo (2020) investigated experimentally the details of heat transfer rate in the generator and absorber, as well as the heat losses, in ARS with 1.5 kW of cooling capacity. Another experimental work from Narváez-Romo *et al.* (2022) analyzed the heat transfer rates in the generator and rectifier. Those studies were developed applying ammonia-water mixture as working fluid pair.

Huirem and Sahoo (2020) investigated the system COP and thermodynamic parameters optimizations in a single effect ARS using water-lithium bromide (H_2O-LiBr) with cooling load of 17.5 kW. The first and second laws of Thermodynamics were employed to model the system. The work of Kadyan *et al.* (2021) presented the simulation of ARS using H_2O-LiBr with 5 kW cooling capacity to study the implementation of an optimizer. Ebrahimnataj Tiji *et al.* (2020) used the commercial software Engineering Equation Solver (EES) and MATLAB to simulate and optimize the start-up time and transient conditions of an ARS using ammonia-water or water-lithium bromide working pairs. The usage of an optimized heat exchanger provided improvement over transient aspects of COP and heat transfer rate in generator and condenser, reducing the start-up time.

Chen *et al.* (2019) simulated an ARS integrated with VCRS only using ammonia-water and R-134a as working fluids, respectively. Herrera-Romero and Colorado-Garrido (2020) compared working fluid pairs to drive a compression-absorption refrigeration system. They analyzed the influence of each heat exchanger with cooling load of 50 kW and temperatures in generator, evaporator, and condenser at 90°C, -10°C, and 40°C, respectively, resulting in COP of 0.36-0.65 for absorption cooling cycle and COP of 6.21-6.62 for vapor compression refrigeration cycle. A method to compare the performance of cooling systems driven by thermal (waste heat, for example) or electrical energy was presented by Rocha *et al.* (2012). It is based on primary energy saving index and could be applied on these integrated systems.

Other studies compared different working pairs from those already exposed using thermodynamic simulation, as the work proposed by Khelifa *et al.* (2021), which correlated their results with system COP. Zhang *et al.* (2021) studied the combination of thermally regenerative batteries based on ammonia with an ARS requiring three different fluids: NH_3/$LiNO_3$/LiBr. The thermodynamic model proved ARS could be powered by these batteries.

Also, the integration of an ARS with other systems is common to work with different thermal energy sources or even to increase the viability and benefits of power generation plants and desalinization systems, for example. Souza *et al.* (2020) developed a model using EES to study the integration of an ARS with organic Rankine cycle, while Hernández-Magallanes *et al.* (2021) investigated the overall COP of a system integrating an ARS (as heat pump and cooling system) with a power generation design. The research developed by Tashtoush and Qaseem (2021) explored the variation of characteristics in an ARS integrated with thermoelectric generator to examine possible optimizations.

Those research results found in open literature do not focus on comparison between absorption and vapor compression cooling systems directly, using the same operating conditions for both and with the same refrigerant fluid. This proposed investigation can be a great tool to verify which system has more benefits in different situations, such as a lower evaporator temperature. In this way, the present work aims to simulate and compare two different types of cooling systems: single stage ammonia-water absorption and vapor compression refrigeration (working with R-134a or R-717). The thermodynamic simulation will be carried out by using the software EES (Engineering Equation Solver). Heat transfer rates of main devices, coefficients of performance for both systems and specific areas of condenser and evaporator will be evaluated.

THERMODYNAMIC MODELS

The proposed single effect absorption refrigeration system works with ammonia-water mixture, while the vapor compression refrigeration system (VCRS) uses R-134a or R-717 (anhydrous ammonia) as refrigerant. The thermodynamic models of these systems were developed with Engineering Equation Solver (EES) and the thermodynamic properties were calculated by the EES standard library. The operating conditions applied for both refrigeration systems are shown in Tab. 1 and the particularities of each one will be described in the upcoming sections.

Table 1. Operating conditions for both refrigeration systems.

Device	Variable or Property	Value
Evaporator	Cooling capacity	15 kW
Condenser outlet	Fluid temperature	40°C
Generator outlet	Vapor temperature	110°C
Evaporator outlet	Vapor temperature	-20°C to 10°C, steps of 5°C

To predict specific areas of condenser and evaporator in the refrigeration systems, two heat exchanger subsystems were assumed: (i) cooling loop for condenser; (ii) thermal load loop of 15 kW for evaporator. Each subsystem was presumed to transfer

heat using a heat exchanger type shell and tube filled with 30% EGW (mixture of 30% ethylene-glycol and 70% water). Subsystems operating conditions are expressed in Tab. 2.

Table 2. Operating conditions for subsystems assumed on both refrigeration systems.

	Subsystem	
Description	**Condenser cooling loop**	**Evaporator thermal load loop**
Working fluid	30% EGW[(1)]	30% EGW[(1)]
Inlet fluid temperature	29°C	+15°C than refrigerant at evaporator inlet
Outlet fluid temperature	34°C	+10°C than refrigerant at evaporator outlet

[(1)] Liquid mixture of 30% ethylene-glycol with 70% water.

Absorption Refrigeration System

The schematic of the single effect absorption refrigeration system (ARS) is presented in Fig. 1. This technology has the main advantage of powering the cooling system with thermal energy, requiring low electrical power. In short, the system was composed by absorber, generator, rectifier, condenser and evaporator, but also includes a pump, two expansion valves and two heat exchangers to work properly. Heat exchangers 1 and 2 were used to improve the performance of this system compared to basic ARS.

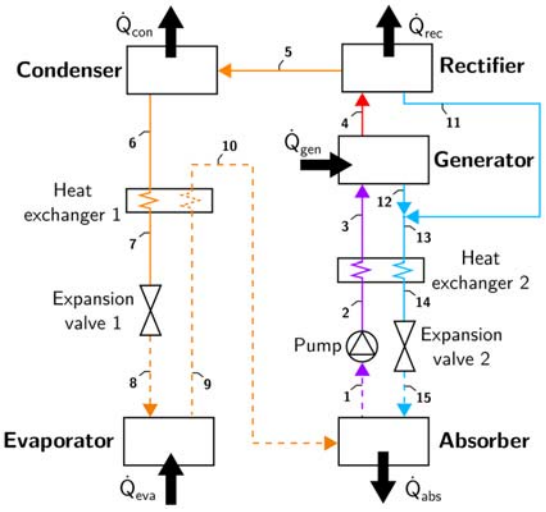

Figure 1. Schematic view of the single effect absorption refrigeration system (ARS).

In Fig. 1, the high pressure sections are shown in full lines and the low pressure segments are in dashed lines. The water-ammonia solutions found in the system have different names based on its ammonia mass fraction: the refrigerant (highlighted in orange in the Fig. 1, from point 5 to 10) has ammonia with high purity degree, the weak solution (blue color, from 11 to 15) has the lowest ammonia mass fraction compared to those three, and the strong solution (purple color, from 1 to 3) has higher ammonia mass fraction than weak solution, but lower than the refrigerant. Those last two solutions are at liquid state in the simulated ARS.

Starting from absorber in Fig. 1, vapor refrigerant coming from evaporator (point 10) is absorbed by the weak solution from generator and rectifier (15), resulting in strong solution (1) and heat generated by absorption process. The strong solution (1) is pumped to the generator (2) through the heat exchanger 2 to increase the fluid temperature (3). In the generator, thermal energy is used to vaporize the ammonia in the strong solution, making vapor at higher ammonia mass fraction (4). To increase ammonia purity heat must be rejected from this fluid in the rectifier to generate the refrigerant (ammonia with high purity degree - point 5), which is liquefied inside the condenser (6). In the heat exchanger 1 the fluid temperature decreases (7) after transferring heat. After, the expansion valve 1, the fluid pressure drops (8) by the Joule-Thomson effect, changing pressure from about 15 bar to approximately 2 bar. In the evaporator, refrigerant vaporizes (9) while absorbing the thermal load. The vapor temperature increases in the heat exchanger 1 (10) and then it flows towards the absorber. Going back to the generator and the rectifier, the weak solution exits from both (11 and 12) and are mixed up (13). Then, the heat exchanger 2 decrease the fluid temperature (14) after transferring heat. The fluid pressure (and temperature) also decreases across the expansion valve 2 (15), and the cycle starts again.

The thermodynamic model was developed applying energy and mass conservation laws on each device. An additional operating condition for ARS was defined: the fluid in the absorber outlet is at 23°C. The mass fraction of strong and weak solutions remained constant in the pump, expansion valve 2 and heat exchanger 2. Expansion valves were isenthalpic, pump was isentropic with 85% of thermodynamic efficiency and heat exchangers were specified with 80% of thermal effectivity. Pressure drops and heat losses in the system were neglected.

Some thermodynamic conditions assumed were defined in the Tab. 3. Energy balance inside heat exchangers was similar, and both require some assumptions. In the heat exchanger 1, refrigerant (ammonia) properties from points 7 and 10 were unknown. First of all, temperatures of these unknown lines were set as the same as strong solution evaporator outlet (9) and condenser outlet (6) temperatures, respectively. Then, their assumed thermodynamic properties were calculated based on the pressure of each segment. The minimum heat capacity rate between the hot and cold fluid within each heat exchanger segment was used to apply the effectiveness-NTU method. Then, the unknown thermodynamic properties were finally predicted.

Table 3. Thermodynamic conditions at the inlet or outlet flow of devices in the ARS.

Point at Fig. 1	Description	Thermodynamic property	Condition
1	Absorber outlet	Vapor quality	Saturated liquid
4	Strong solution generator outlet	Vapor quality	Saturated vapor
5	Condenser inlet	Vapor quality	Saturated vapor
6	Condenser outlet	Ammonia mass fraction	Pure ammonia
		Vapor quality	Saturated liquid
9	Evaporator outlet	Ammonia mass fraction	Pure ammonia
		Vapor quality	Saturated vapor
11	Weak solution rectifier outlet	Vapor quality	Saturated liquid
		Temperature	Average between points (4) and (5)
12	Weak solution generator outlet	Vapor quality	Saturated liquid

Thermodynamic simulation brought as results the pump power, the dissipated heat rates in the rectifier, condenser and absorber, and the heat rate necessary to drive the generator. All of them were calculated based on assumptions already described. The coefficient of performance (COP) of this absorption refrigeration system was determined by Eq. (1):

$$COP_{ARS} = \frac{\dot{Q}_{eva}}{\dot{Q}_{gen}} \quad (1)$$

where $\dot{Q}_{eva}$ is the refrigeration thermal load (15 kW, as mentioned before), kW, and $\dot{Q}_{gen}$ the heat transfer rate to generator, kW.

Heat exchanger areas of condenser, including the rectifier, and evaporator were calculated based on logarithmic mean temperature difference and assuming countercurrent flow in the subsystems heat exchangers. The operating conditions were described in the Tab. 2. Condensation and rectifier areas were analyzed together because other absorption refrigeration systems do not have a rectifier. The global heat transfer coefficients used were the average values proposed by BRASIL (2017) for anhydrous ammonia, also known as R-717 refrigerant: 2.1 kW/m^2.K for condenser (or rectifier) and 1.9 kW/m^2.K for evaporator. The specific area, then, was defined by Eq. (2):

$$A_{esp} = \frac{A_{dev}}{\dot{Q}_{eva}} \quad (2)$$

where A_{esp} is the specific area, m²/kW, and A_{dev} the heat exchanger area from condenser (with rectifier) or evaporator, m².

Vapor Compression Technology

The VCRS simulated is shown in Fig. 2. In the evaporator, refrigerant vaporizes (point 1) as it absorbs the thermal load and is redirected towards compressor. Electrical power is given to compress the R-134a or R-717 refrigerant (2) that is driven to the condenser to decrease the fluid temperature to the liquid state (3). The expansion valve is used to decrease the fluid pressure and consequently the temperature before entering into the evaporator (4). In the Fig. 2, the high pressure sections are shown in full lines and the low pressure segments are in dashed lines.

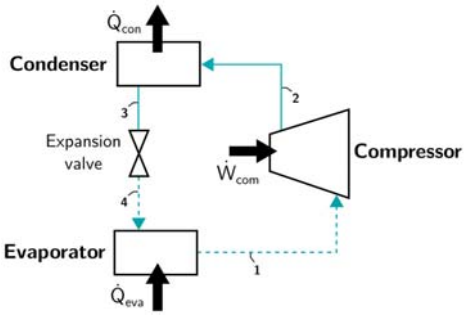

Figure 2. Schematic view of the vapor compression refrigeration system (VCRS).

The VCRS thermodynamic model was similar to the ARS one and was developed applying energy and mass conservation laws on each device. Initial conditions were defined as shown in Tab. 1. Pressure drops and heat losses from the system were neglected, and compressor was assumed isentropic and working with 85% of thermodynamic efficiency. Some assumed thermodynamic conditions are defined in Tab. 4.

Table 4. Thermodynamic conditions at the inlet or outlet flow of devices in the VCRS.

Point at Fig. 1	Description	Thermodynamic property	Condition
1	Evaporator outlet	Vapor quality	Saturated vapor
		Temperature	The same as evaporator inlet
3	Condenser outlet	Vapor quality	Saturated liquid

Thermodynamic simulation gave as results the compressor power and the dissipated heat rate in the condenser. All of them were calculated based on assumptions already described. The VCRS COP was determined by Eq. (3):

$$COP_{VCRS} = \frac{\dot{Q}_{eva}}{\dot{W}_{com}} \quad (3)$$

where $\dot{Q}_{eva}$ is the refrigeration thermal load (15 kW, as mentioned before), kW, and $\dot{W}_{com}$ the compressor power required to drive the system, kW.

Condenser and evaporator heat exchanger areas were calculated based on logarithmic mean temperature difference and assuming countercurrent flow in the subsystems heat exchangers. Thermodynamic conditions were described in the Tab.

2. The global heat transfer coefficients used were the average values proposed by BRASIL (2017). Using R-134a refrigerant those numbers were 1.6 kW/m^2.K for condenser and 0.9 kW/m^2.K for evaporator, while using R-717 those values were 2.1 kW/m^2.K for condenser and 1.9 kW/m^2.K for evaporator. The specific area, then, was defined by Eq. (2).

RESULTS AND DISCUSSION

Figure 3 shows heat transfer rates in the main devices and presents the ARS Coefficient of Performance (COP). Comparisons were related to the decrease of evaporator temperature. The generator heat rate necessary to drive the ARS increased from 25.0 kW to 41.8 kW as absorber heat dissipated in the environment also increased from 19.2 kW to 36.7 kW. The heat transfer rate of condenser and rectifier remained almost constant, between 14.2-14.4 kW and 6.30-6.38 kW, respectively, while COP decreased from 0.601 to 0.359. The specific areas (area per kW of refrigeration load - kWr) are demonstrated in the Fig. 4. Condenser (with rectifier) and evaporator specific areas remained almost the same, changing between 0.0788-0.0798 m^2/kWr and 0.0423-0.0426 m^2/kWr, respectively.

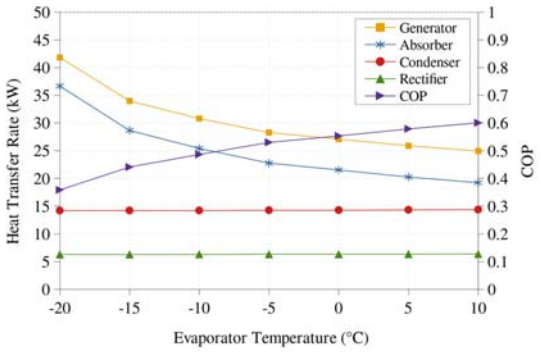

Figure 3. Heat transfer rates of ARS devices for different evaporator temperatures.

Compressor power and condenser heat rate dissipation required for VCRS are presented by Fig. 5. Working with R-134a refrigerant, as evaporator temperature decreased, compressor power increased from 2.22 kW to 5.76 kW and condenser heat dissipation increased from 16.9 kW to 19.9 kW. Using the same comparison parameter, COP decreased from 6.77 to 2.60. Fig. 6 indicates that condenser specific area decreased from 0.0700 to 0.0649 m2/kWr, while evaporator specific area remained at 0.0901 m2/kWr.

For the system working with R-717, the values were slightly different. As evaporator temperature decreased, compressor power increased from 2.12 kW to 5.38 kW, condenser heat dissipation increased from 16.8 kW to 19.6 kW, and COP decreased from 7.07 to 2.79. Fig. 6 indicates that condenser specific area decreased from 0.0228 to 0.0152 m^2/kWr, while evaporator specific area remained at 0.0427 m^2/kWr.

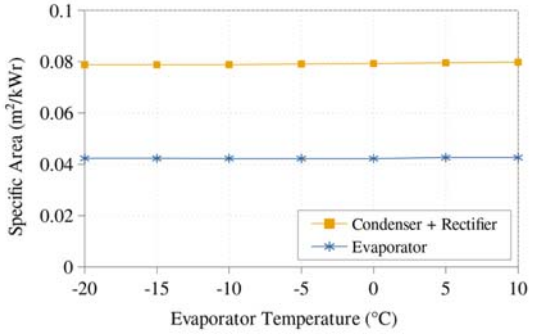

Figure 4. Condenser (with rectifier) and evaporator specific areas of ARS for different evaporator temperatures.

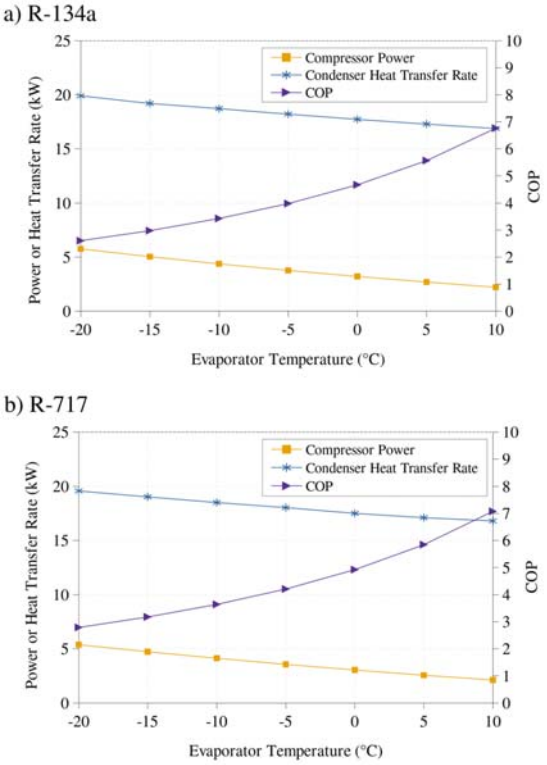

Figure 5. Compressor power, condenser heat transfer rate and COP of devices from VCRS for different evaporator temperatures using: (a) R-134a, and (b) R-717.

The results for VCRS using R-134a or R-717 had minor changes, and hereafter they were mentioned together, with (lower value) – (higher value) standard. When considerable changes were found they were indicated and analyzed individually as an exception. Comparing the two cooling systems, as evaporator temperature reduced from 10°C to -20°C, COP for

ARS decreased by 40.3%, while VCRS decreased 60.6-61.5%, which means ARS COP was less susceptible to evaporator temperature, even when comparing the systems working with the same refrigerant. However, VCRS COP were an average of 10 times higher than ARS COP. For both systems, the COP calculated using this thermodynamic model were similar to those found by Hmida *et al.* (2019) and Herrera-Romero and Colorado-Garrido (2020).

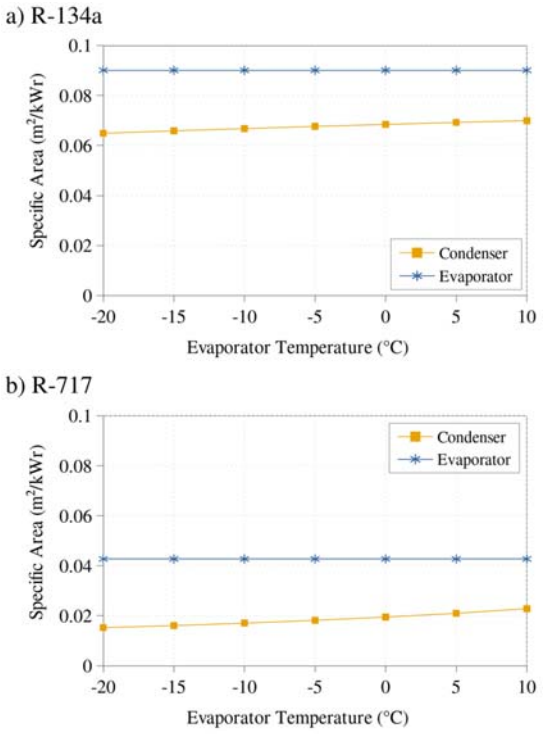

Figure 6. Condenser and evaporator specific areas of VCRS for different evaporator temperatures using: (a) R-134a, and (b) R-717.

Generator heat transfer rate for ARS had an expressive increase of 16.9 kW, or 67.5%, while compressor power for VCRS raised 3.26-3.54 kW, or 154-160%. Although these percentages were high for VCRS the raw values were far lower than ARS. Comparing the heat transfer rates needed to be dissipated, VCRS condenser had an increment of 2.77-3.02 kW or 17.9% and the ARS absorber increased 17.4 kW or 90.5%. Note that the condenser and rectifier heat transfer rates for ARS remained almost constant due to the operating and thermodynamic conditions, which did not change the thermodynamic states at points (4), (5), (6) and (11). In other words, temperatures, pressures and vapor qualities were the same in these points when evaporator was at 10°C to -20°C. Consequently, the increase in the generator heat transfer rate increased the mass flow rate of strong and weak solution up to 8 and 15 times, respectively.

The high numbers of heat rates and low COPs of absorption refrigeration system can be a challenge in the implementation of this technology, meaning this type of cooling system has more advantages when employed in locations with high amounts of waste heat. This way many industries can use waste heat sources instead of electrical power to drive their cooling systems.

According to variations of evaporator temperature, ARS specific areas changed up to 1.2% as shown in Fig. 4 because heat transfer rates at condenser and rectifier had little changes in their thermodynamic conditions and the inlet and outlet of condenser cooling subsystem were at constant temperature. The VCRS required specific areas to change up to 7.5% according to Fig. 6. The only exception was the condenser specific area of VCRS using R-717 that changed 33.2% due to the high increase of ammonia temperature difference between inlet and outlet of condense (variation from 36.6 K to 95.5 K). This high raise in temperature difference in the condenser was not present on the other systems studied even using equal operating conditions.

Analyzing VCRS specific areas when working with R-134a, condenser was 14.7% smaller in average and evaporator around two times smaller compared to ARS. For VCRS using R-717 (ammonia), the same refrigerant used by ARS, specific areas for condenser were around 76.6% smaller (1/4 of specific size) while evaporator was required to have the same specific size.

Little or no differences in specific areas for condenser from ARS and evaporator from both systems happened because global heat transfer rate and thermal load for evaporator were the same, heat exchanger types were equal and temperature difference at inlet and outlet changed very little. In summary, specific areas were mainly related to heat transfer coefficients that depend on the refrigerant and heat exchanger type used.

CONCLUSIONS

The proposed thermodynamic simulation for both refrigeration systems, a single effect absorption working with ammonia-water and a vapor compression using R-134a or R-717 (anhydrous ammonia), were carried out based on energy and mass conservation laws with assumed operational and thermodynamic conditions. Overall, ARS thermal power required was greater than VCRS electrical power. The results of ARS COP were between 0.359-0.601, while VCRS reached between 2.60-6.77 for R-134a and 2.79-7.07 for R-717. Those numbers were similar to other works found in literature and they can, in a future work, be evaluated using the methodology presented by Rocha *et al.* (2012) to equal residual thermal energy with electricity.

As evaporator temperature decreased, absorption refrigeration system (ARS) required up to 16.9 kW, or 67.5%, more heat rate in generator, but must dissipate 17.4 kW or 90.5% more heat rate in absorber. COP decreased by up to 40.3% and heat transfer rates of

condenser and rectifier did not have considerable changes. Using the same comparison parameter, the vapor compression refrigeration system (VCRS) needed up to 3.26-3.54 kW, or 154-160%, more compressor power and COP decreased up to 60.6-61.5%. Compared to ARS, condenser specific area required for VCRS was smaller, evaporator could be twofold smaller when using R-134a, and needed to have equal size when using R-717. The calculated specific areas proved to be highly dependent on the type of refrigerant and heat exchanger.

In summary, ARS had higher increase of generator heat input rate compared to compressor power in the VCRS, as evaporator temperature decreased. The opposite trend was observed when comparing the COP, which means ARS COP changed less than in VCRS when working with the same evaporator temperature variation and refrigerant. The raw values, however, were higher for the VCRS. The characteristics of absorption refrigeration systems presented here enhance the advantages of this cooling technology when used in industries or facilities with high amounts of waste heat, saving electrical power mainly at lower evaporator temperatures.

ACKNOWLEDGEMENTS

This study was financed in part by the Coordenação de Aperfeiçoamento de Pessoal de Nível Superior – Brasil (CAPES) - Finance Code 001. The third author thanks to Fundação de Apoio à Universidade de São Paulo (FUSP) for the scholarship, n. 23536725821/2022, and the Thematic Project financing, 2016/09509-1 – (FAPESP), as well as the Colombian Administrative Department of Science, Technology and Innovation - Minciencias - (COLCIENCIAS grant 1.087.046.934-728/2015).

REFERENCES

Braga Martins, K.R.S. and Figueiredo, J.R., 2019. "Computational simulation and optimization methodology of an ammonia–water GAX absorption cooling system". Journal of the Brazilian Society of Mechanical Sciences and Engineering, Vol. 41, No. 11, p. 507.

BRASIL, 2017. *Ar condicionado : manual sobre sistemas de água gelada : conceitos sobre chillers e sistemas de água gelada.* Ministério do Meio Ambiente. Secretaria de Mudança do Clima e Florestas. Departamento de Monitoramento, Apoio e Fomento de Ações em Mudança do Clima, Brasília, DF.

Chen, W., Li, Z., Sun, Q. and Zhang, B., 2019. "Energy and exergy analysis of proposed compression-absorption refrigeration assisted by a heat-driven turbine at low evaporating temperature". Energy Conversion and Management, Vol. 191, pp. 55–70.

Ebrahimnataj Tiji, A., Ramiar, A. and Ebrahimnataj, M., 2020. "Comparison the start-up time of the key parameters of aqua-ammonia and water–lithium bromide absorption chiller (AC) under different heat exchanger configurations". SN Applied Sciences, Vol. 2, No. 9, p. 1522.

Hernández-Magallanes, J.A., Tututi-Avila, S., Cerdán-Pasarán, A., Morales, L.I. and Rivera, W., 2021. "Thermodynamic simulation of an absorption heat pump-transformer-power cycle operating with the ammonia-water mixture". Applied Thermal Engineering, Vol. 182, p. 116174.

Herrera-Romero, J.V. and Colorado-Garrido, D., 2020. "Comparative Study of a Compression–Absorption Cascade System Operating with NH3-LiNO3, NH3-NaSCN, NH3-H2O, and R134a as Working Fluids". *Processes*, Vol. 8, No. 7, p. 816. Number: 7 Publisher: Multidisciplinary Digital Publishing Institute.

Hmida, A., Chekir, N., Laafer, A., Slimani, M.E.A. and Ben Brahim, A., 2019. "Modeling of cold room driven by an absorption refrigerator in the south of Tunisia: A detailed energy and thermodynamic analysis". Journal of Cleaner Production, Vol. 211, pp. 1239–1249.

Huirem, B. and Sahoo, P.K., 2020. "Thermodynamic Modeling and Performance Optimization of a Solar-Assisted Vapor Absorption Refrigeration System (SAVARS)". *International Journal of Air-Conditioning and Refrigeration*, Vol. 28, No. 01, p. 2050006. Publisher: World Scientific Publishing Co.

Kadyan, H., Berwal, A.K. and Mishra, R.S., 2021. "Thermodynamic mathematical modelling and analysis of vapour absorption refrigeration system using a novel ant lion optimiser". International Journal of Ambient Energy, Vol. 0, No. 0, pp. 1–14. Taylor & Francis.

Kassas, M., 2015. "Modeling and Simulation of Residential HVAC Systems Energy Consumption". Procedia Computer Science, Vol. 52, pp. 754–763.

Khelifa, S., Ramadan, K., Ammar, M.A.H. and Moundji, H.M., 2021. "Performance evaluation of an absorption refrigeration system using R1234yf - organic absorbents working fluids". Science and Technology for the Built Environment, Vol. 0, No. 0, pp. 1–18. Taylor & Francis.

Narváez-Romo, B., 2020. An experimental study of an ammonia-water absorption refrigeration cycle using a novel modified horizontal liquid film absorption system. Doctoral Thesis, Graduate Program in Mechanical Engineering, Escola Politécnica, University of São Paulo, São Paulo, Brazil.

Narváez-Romo, B., Chhay, M., Zavaleta-Aguilar, E.W. and Simões-Moreira, J.R., 2017. "A critical review of heat and mass transfer correlations for LiBr-H2O and NH3-H2O absorption refrigeration machines using falling liquid film technology".

Applied Thermal Engineering, Vol. 123, pp. 1079–1095.

Narváez-Romo, B., Leite, B.M. and Simões-Moreira, J.R., 2020. "Ammonia-water absorption process on falling films at vertical and inclined plates". *Heat Transfer Research*, Vol. 51, No. 4, pp. 297–318.

Narváez-Romo, B. and Simões-Moreira, J.R., 2019. "Numerical study of heat and mass transfer absorption processes using a horizontal flooded-liquid film in ammonia-water mixtures." In *Proceedings of the 25th IIR International Congress of Refrigeration*. IJR, Montréal, Canada, p. 1269.

Narváez-Romo, B., Zavaleta-Aguilar, E.W. and Simões-Moreira, J.R., 2022. "Heat and mass transfer in falling films technology applied to the generator and the rectifier of an ammonia-water absorption refrigeration cycle". International Journal of Refrigeration, Vol. 135, pp. 276–287. ISSN 0140-7007.

Opoku, R., Edwin, I.A. and Agyarko, K.A., 2019. "Energy efficiency and cost saving opportunities in public and commercial buildings in developing countries – The case of air-conditioners in Ghana". Journal of Cleaner Production, Vol. 230, pp. 937–944.

Rocha, M., Andreos, R. and Simões-Moreira, J. R., 2012. "Performance tests of two small trigeneration pilot plants". Applied Thermal Engineering, Vol. 41, pp. 84–91.

Souza, R.J., Dos Santos, C.A.C., Ochoa, A.A.V., Marques, A.S., Neto, J.L.M. and Michima, P.S.A., 2020. "Proposal and 3E (energy, exergy, and exergoeconomic) assessment of a cogeneration system using an organic Rankine cycle and an Absorption Refrigeration System in the Northeast Brazil: Thermodynamic investigation of a facility case study". Energy Conversion and Management, Vol. 217, p. 113002.

Tashtoush, B. and Qaseem, H., 2021. "An integrated absorption cooling technology with thermoelectric generator powered by solar energy". Journal of Thermal Analysis and Calorimetry.

Wells, J. and Haas, D., 2004. *Electricity Markets: Consumers Could Benefit from Demand Programs, But Challenges Remain.* DIANE Publishing.

Zhang, S., Luo, J., Xu, Y., Chen, G. and Wang, Q., 2021. "Thermodynamic analysis of a combined cycle of ammonia-based battery and absorption refrigerator". Energy, Vol. 220, p. 119728.